PCCP

Factors affecting cyclic durability of all-solid-state lithium batteries using poly(ethylene oxide)-based polymer electrolytes and recommendations to achieve improved performance

Journal:	*Physical Chemistry Chemical Physics*
Manuscript ID	CP-ART-08-2018-005440.R1
Article Type:	Paper
Date Submitted by the Author:	24-Sep-2018
Complete List of Authors:	Faglioni, Francesco ; University of Modena and Reggio Emilia, Department of Chemical and Geological Sciences Merinov, Boris; CALTECH, Beckman Institute, Center for Materials and Molecular Simulation Goddard, William; CALTECH, Beckman Institute, Center for Materials and Molecular Simulation Kozinsky, Boris; Harvard University, Paulson School of Engineering and Applied Sciences

Journal Name

ARTICLE TYPE

Cite this: DOI: 10.1039/xxxxxxxxxx

Factors affecting cyclic durability of all-solid-state lithium batteries using poly(ethylene oxide)-based polymer electrolytes and recommendations to achieve improved performance†

Francesco Faglioni,*[a] Boris V. Merinov,[b] William A. Goddard III,[b] and Boris Kozinsky[c]

Received Date
Accepted Date

DOI: 10.1039/xxxxxxxxxx

www.rsc.org/journalname

A detailed experimental analysis of the factors affecting cyclic durability of all-solid-state lithium batteries using poly(ethylene oxide)-based polymer electrolytes was published in EES by Nakayama et al. We use quantum mechanics to interpret these results, identifying processes involved in the degradation of rechargeable lithium batteries based on polyethyleneoxyde (PEO) polymer electrolyte with LiTFSI. We consider that ionization of the electrolyte near the cathode at the end of the recharge step is probably responsible for this degradation. We find that an electron is likely removed from PEO next to a TFSI anion, triggering a sequence of steps leading to neutralization of a TFSI anion and anchoring of another TFSI to the PEO. This decreases the polymer conductivity near the cathode, making it easier to ionize additional PEO and leading to complete degradation of the battery. We refer to this as the Cathode Overpotential Driven Ionization of the Solvent (CODIS) model. We suggest possible ways to confirm experimentally our interpretation and propose modifications to suppress or reduce electrolyte degradation.

1 Introduction

Rechargeable lithium batteries have become an essential part of everyday life in our society, but major improvements in their performance are critical to achieve their full technological and economic impact. Many reviews of lithium batteries are available in literature (see for instance Ref.[1].)

One critical issue is to reduce their weight, to make applications to transportation economic. A possible solution is to use metallic lithium as an electrode, the so-called lithium-metal batteries (LMBs), instead of the lithium-ion batteries (LIBs) currently on the market. In fact, LMBs have the theoretical potential of providing the same capacity as LIBs but with a total weight 5 to 10 times smaller, making LMB ideal candidates for automobile applications. Unfortunately, the development of LMBs is hampered by severe technical and scientific problems, mainly tied to the extreme reactivity of metallic lithium and to its extremely small surface energy. Thus, metallic lithium can only be in contact with particularly stable electrolytes and tends to form dendrites upon recharging of the cell. The dendrites quickly grow through liquid electrolytes, reach the other electrode and short-circuit the battery, leading to irreversible damage and serious safety issues. A promising solution to prevent or reduce this problem is to cover the metal surface with a Li-ion conducting solid polymer electrolyte (SPE), instead of a liquid one.

In this case, a most promising polymer is polyethylene oxide (PEO). When coupled with Li salts containing large anions and, sometimes, smaller additives acting as plasticizer, PEO provides high enough Li-ion conductivity, and both good chemical and mechanical properties. Commonly used salts are LiTFSI or $LiPF_6$, where TFSI is the acronym for Bis(trifluoromethane)sulfonimide anion.

TFSI: 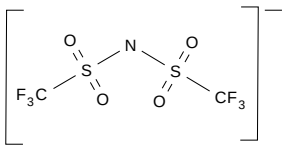

(1)

Using the PEO-LiTFSI electrolyte, it is possible to build LMBs capable of maintaining a good electrical capacity for tens or hundreds of charge/discharge cycles under controlled laboratory con-

[a] Department of Chemical and Geological Sciences, University of Modena e Reggio Emilia, Via Campi 103, 41125 Modena, Italy. Tel: +39 059 205 8546; E-mail: francesco.faglioni@unimore.it
[b] Materials and Process Simulation Center, California Institute of Technology, Pasadena, CA 91125, USA.
[c] John A. Paulson School of Engineering and Applied Sciences, Harvard University, Cambridge, MA 02138, USA.

† Electronic Supplementary Information (ESI) available: Discussion of DFT functionals and the role of exact HF exchange in charge delocalization and Self Interaction Correction. See DOI: 10.1039/b000000x/

ditions.[1] Of course far longer lifetimes are required for technological applications. Hence, it is important to understand what causes degradation of LMBs in order to develop strategies to increase dramatically their average operative life.

Since LMBs are rather complex systems, from both theoretical and experimental perspectives, it is essential to analyze them using a variety of diagnostic techniques and combine the results to provide a more complete description of battery behavior. Thus, we use quantum mechanics (QM) to provide first principles interpretations of the experimental results and a fundamental understanding of the chemistry for these systems.

Nakayama et al.[2,3] reported in EES experimental results on cell degradation for PEO-LiTFSI systems that they investigated using a combination of electrochemical techniques, including NMR imaging and pressure tests. We apply our QM methods to interpret their results in terms of the fundamental processes, which we summarize briefly.

Nakayama et al.[3] used metallic lithium anodes and cathodes made of $LiFePO_4$ (active material), acetylene black (electrical conductor), and $LiClO_4$/PEO (binder and $Li^{\oplus}$ conductor.) For these systems, they report the following.

1. Cell properties change upon the first charge/discharge cycle, but then remain essentially constant for many cycles, until degradation initiates.

2. Degradation begins near a critical event, termed "trigger-point", which occurs after a different number of cycles for each cell, but it appears to develop according to the same electrochemical pattern.

3. A few (5-10) cycles before the trigger point, the electrical resistance at the Anode/SPE interface (R_{ia}) starts to decrease.

4. Starting at the trigger point, the electrical resistance at the Cathode/SPE interface (R_{ic}) grows rapidly, leading to battery failure.

5. The trigger point is not correlated to the time spent by the system at different voltages.

6. Following degradation, fluorine (from TFSI) is largely localized near specific points at the Cathode/Electrolyte interface.

7. Pressure studies seem to indicate that degradation is related to defects in the contact between cathode and electrolyte, that is, to the reduced contact area that leads to increased resistance R_{ic} and hence to a larger potential drop in this region.

8. These results suggest that degradation may start at the end of the recharge step, when the cathode is positively charged, the applied potential is 3.8 V, and $TFSI^{\ominus}$ tends to be near the cathode.

Analyzing the resistances at the Cathode/SPE (R_{ic}), at the Anode/SPE (R_{ia}), and associated to the bulk electrolyte (R_b) as measured by Nakayama et al. and reported in Figure 1, and assuming a cell potential of 3.8 V, we derive the voltage drops before

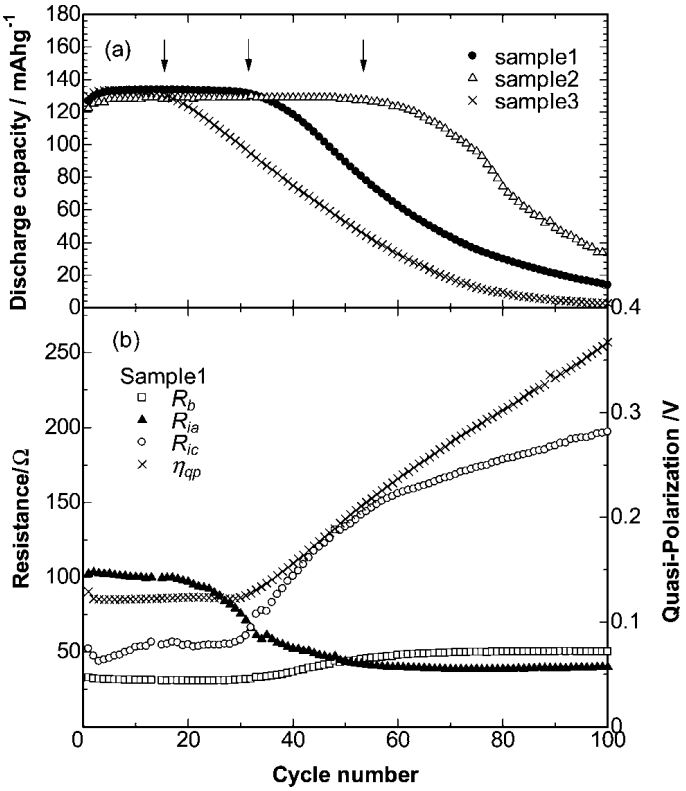

Fig. 1 Fig. 4 from Ref.[3]. (a) Cyclic performance for three LPBs (Samples 1-3) composed of the same materials and identically constructed. Arrows indicates trigger points. (b) Variation of internal resistances R_b , R_{ia} , and R_{ic} , and quasi-polarization η_{qp} with cycling.
Reproduced from Ref.[3] with permission from the Royal Society of Chemistry.

Table 1 Resistance and potential drop ΔV for each region of the battery before degradation and at the trigger point

		Resistance (Ω)[a]		$\Delta V(V)$[b]	
Site	Name	Before degr.	Trigger point	Before degr.	Trigger point
Cathode/SPE	R_{ic}	50	50	1.06	1.27
Anode/SPE	R_{ia}	100	70	2.11	1.77
Bulk	R_b	30	30	0.63	0.76

[a] From ref.[3].
[b] Estimates based on a battery potential of $3.8\,V$.

and at the trigger point reported in Table 1. Hence, we associate degradation with the ΔV increase from 1.06 to 1.27 V at the Cathode/SPE interface.

In the Ref.[3] the cathodes are based on $LiFePO_4$ deposited on acetylene black, but similar degradations have been reported also for other electrodes, such as Pt, Ni, metal oxides, and stainless steel.[4] This suggests that the degradation process does not depend on the chemical nature of the cathode surface.

We investigate here the possible electrochemical decomposition of $TFSI^{\ominus}$ or PEO at the end of the recharge step. This possibility depends on the ionization potential (IP) for $TFSI^{\ominus}$ and PEO. Hence, it is essential to use a computational method appropriate to describe ionization of anions and their coordinating solvent molecules or polymer fragments.

1.1 Computational details

All computations were performed using the commercial program `Gaussian09`[5], with the 6-311++G** basis set[6,7] on all atoms. Computations are carried out in diethylether, treated as implicit solvent[8] as implemented in `Gaussian09`. This solvent has a dielectric constant $\varepsilon = 4.24$, similar to that of PEO.

Electron transfer (ET) energies are computed treating the cathode as a reservoir of electrons with energy

$$E^c_{el} = \varepsilon_F - \Delta V,$$

where ε_F is the Fermi energy for the cathode (taken as a negative value), and ΔV is the applied bias, accounting for the voltage drop between cathode and electrolyte. So, for a generic ET process from species A, within the electrolyte, to the cathode, the energy is $\Delta E = E(A^{\oplus}) + E^c_{el} - E(A)$.

Computationally, this is equivalent to shifting the potential energy surface for the ionized state by the fixed amount E^c_{el}. All ΔE reported in this article refer to the optimized geometries for both reactants and products.

We do not know the Fermi energy for $LiFePO_4$, but for other electrodes (Pt, Ni) for which the work functions are available[9], ε_F are below $-5\ eV$. Also, $LiFePO_4$ is supported on acetylene black, a high porosity conductive carbon, for which $\varepsilon_F \approx -5.0\ eV$ (from the C work function[9].) Thus we will assume $\varepsilon_F = -5.0\ eV$.

We also compute activation energies E_a based on the same principle. In this case, however, the transition state geometry corresponds to the Minimal Energy Crossing Point (MECP) between the potential energy surfaces for the reduced and oxidized states, where the latter is shifted to account for E^c_{el}.

Algorithms to locate the MECP between two potential energy surfaces, based either on Lagrange multipliers[10,11] or functionals of the energies and gradients[12,13] have been available for several decades, and they have been extensively used to study transitions between different spin surfaces, or excited states with different symmetries. The key requirement is that the two potential energy surfaces must correspond to orthogonal states. We note that locating MECPs between orthogonal states is a minimization problem, and it is both in principle and in practice simpler than finding saddle points for reactions that do not involve orthogonal states.

For the present study, we adapted the code developed by Harvey to locate MECP for transitions between different spin states.[13] Let E_i and $\overline{\nabla}_i$ be the energies and gradients, respectively, of the two states ($i = Red, Ox$), $\overline{X} = \overline{\nabla}_{Red} - \overline{\nabla}_{Ox}$ indicate the difference between gradients, and $\overline{N} = \overline{X}/|X|$ its normalized direction. A new effective gradient is obtained from two orthogonal components:

$$\overline{f} = (E_{Red} - E_{Ox} + E^c_{el})\overline{X} \quad (2)$$

$$\overline{g} = \overline{\nabla}_{Red} - \left(\overline{\nabla}_{Red} \cdot \overline{N}\right)\overline{N}. \quad (3)$$

These are constructed so that, near the MECP, $\overline{f}$ and $\overline{g}$ are orthogonal and parallel, respectively, to the seam, or the crossing hyperline, between the two surfaces, and

- $\overline{f}$ vanishes where the two surfaces cross, and
- $\overline{g}$ vanishes at stationary points along the seam.

Thus, minimization based on the effective gradient

$$\overline{\nabla}_{MECP} = \overline{f} + \overline{g} \quad (4)$$

leads to the desired MECP geometry and energy. We note that both position and energy of the MECP depend on the energy of the electron on the cathode, E^c_{el}. Hence, different optimizations must be performed for different values of E^c_{el}.

The reported activation energies refer to the potential energy required to distort the reactant to a geometry where its energy matches that of the product, i.e., where ET can occur. It does not include the ET Hamiltonian, so it is not sufficient to determine ET rates. These depend also on the overlap between the electronic wavefunction of the reduced state with that for the electron on the cathode, which in turn depends on the distance from the cathode surface. We do not consider this term in this article.

In the ESI and in Ref.[14] we analyze various ways to apply QM methods to the problem and conclude that only DFT functionals with exact HF exchange at long range provide the correct qualitative description of the oxidation process. Hence, our computations are based on M06-HF[15,16] and LC-BLYP[17,18], two forms of non local density functionals. Although these two methods provide slightly different quantitative estimates for reaction and activation energies, they both lead to the same reaction mechanism.

PEO was modeled using one or more explicit molecules of dimethoxyethane (DME).

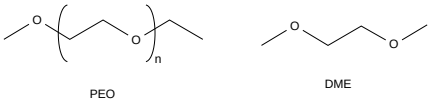

Results

As shown below, degradation of the electrolyte involves the removal of one H atom from DME. Hence, we use the label HPol for DME and $Pol^{\odot}$ and $Pol^{\oplus}$ to indicate the radical and cation obtained from DME upon removal of a hydrogen or a hydrogen with an electron, respectively.

Assuming that the conditions near the cathode lead to ionization of the system, we show in the ESI and in Ref.[14] that the

electron is transferred from DME, which is our model for PEO. Next, we envision the degradation process as follows.

First Electron Transfer

The reaction energy ΔE and activation energy E_a for the first electron transfer from the electrolyte to the cathode depends on the potential energy difference ΔV between cathode and electrolyte. This difference depends on the history and operating conditions of the battery and is not easily accessible. But based on the discussion in the previous section we expect it to

- be at most $\Delta V = 1.06\,V$ before the trigger point,
- increase to an average value no greater than $\Delta V = 1.27\,V$ at the trigger point, and
- keep increasing after degradation has begun.

This potential difference is likely spread across the double layer at the cathode surface, but there may be localized microscopic regions, e.g., tips extruding from the cathode surface, where its value could conceivably be larger than the values just mentioned. Thus, the actual ΔV between a $TFSI^{\ominus}$ anion near the cathode and the cathode itself may be smaller or larger than the two values that we take as reference. Keeping this in mind, we discuss the reaction using

- $\Delta V = 1.06\,V$ for a working battery and
- $\Delta V = 1.27\,V$ for the trigger point

and warn the reader that actual values may differ somewhat, in either direction. This only affects reaction steps that involve electron transfer.

We also show in the ESI and in Ref.[14] that upon the first ET, a radical cation $HPol^{\oplus}$ is formed next to $TFSI^{\ominus}$. The fact that the polymer is oxidized despite having a higher ionization potential than $TFSI^{\ominus}$ is due to electrostatic stabilization of the oxidized form, where the newly formed cation is close to the anion.

This radical character is essentially localized on one oxygen atom and the positive charge is split between the radical oxygen and one of the hydrogens, directed towards the $TFSI^{\ominus}$ nitrogen. The ionized state relaxes spontaneously by transferring $H^{\oplus}$ to the N of $TFSI^{\ominus}$, forming a neutral molecule of HTFSI, which is an extremely strong acid, coordinated to $Pol^{\odot}$.

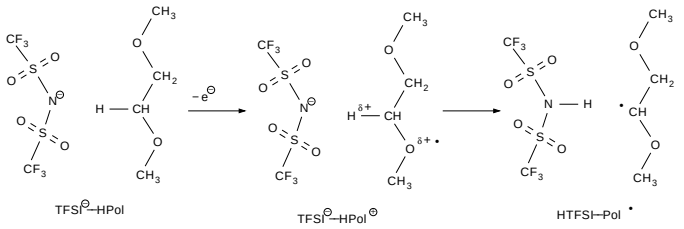

For this combined step, we compute the following activation energies

	before TP	at TP
M06-HF :	$E_a = 1.06\,eV$	$E_a = 0.90\,eV$
LC-BLYP :	$E_a = 0.92\,eV$	$E_a = 0.75\,eV$

and reaction energies

	before TP	at TP
M06-HF :	$\Delta E = 0.17\,eV$	$\Delta E = -0.04\,eV$
LC-BLYP :	$\Delta E = 0.22\,eV$	$\Delta E = 0.01\,eV$

As mentioned above, these activation energies are not sufficient to determine ET rates. Nevertheless, these E_a and ΔE values indicate that ET is plausible at room temperature and that the ET is close to being favorable at the trigger point.

Next, the reaction could follow two paths.

Path 1: Second ET and migration.

It is possible to remove a second electron from the system. This step is energetically extremely favorable and is expected to have significantly lower activation energy than the first ionization,

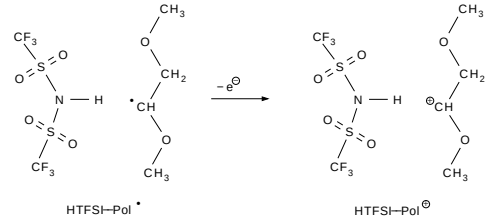

	before TP	at TP
M06-HF :	$E_a = 0.10\,eV$	$E_a = 0.07\,eV$
LC-BLYP :	$E_a = 0.05\,eV$	$E_a = 0.02\,eV$

	before TP	at TP
M06-HF :	$\Delta E = -0.81\,eV$	$\Delta E = -1.02\,eV$
LC-BLYP :	$\Delta E = -1.17\,eV$	$\Delta E = -1.38\,eV$

Since the transfer is easier for this second step, we expect that if the conditions are suitable for the first ET, they will certainly be sufficient for the second ET as well.

Following the second ET, the neutral molecule HTFSI conceivably diffuses away from the corrupted polymer $Pol^{\odot}$ to a pristine site HPol.

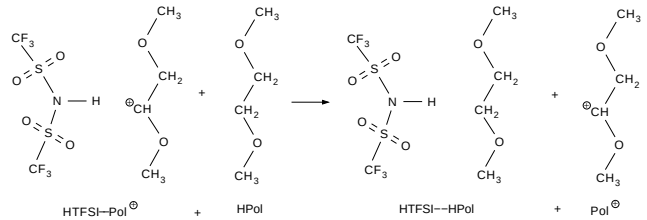

M06-HF : $\Delta E = -0.62\,eV$
LC-BLYP : $\Delta E = -0.29\,eV$

leading to neutralization of a $TFSI^{\ominus}$ anion, which is turned into HTFSI, and the formation of a carbocation on the polymer, modeled as $Pol^{\oplus}$.

Path 2: Migration and second ET.

Alternatively, the HTFSI produced by the first ET could diffuse before the second ET from the radical $Pol^{\odot}$.

In fact, migration is favorable:

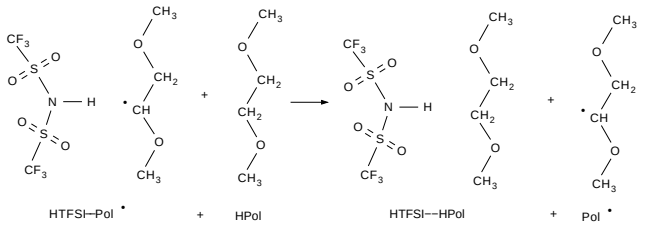

$$\text{M06-HF}: \quad \Delta E = -0.20\ eV$$
$$\text{LC-BLYP}: \quad \Delta E = -0.36\ eV$$

and so is ET from Pol$^{\odot}$. In this case, ET is favorable even at the reactant's geometry, so the electron can transfer directly from the reactant to the electrode's conduction band with vanishing activation energy due to geometric rearrangement

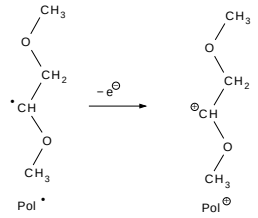

	before TP	at TP
M06-HF:	$\Delta E = -1.24\ eV$	$\Delta E = -1.45\ eV$
LC-BLYP:	$\Delta E = -1.10\ eV$	$\Delta E = -1.31\ eV$

leading to the same HTFSI molecule and carbocation Pol$^{\oplus}$ as in Path 1.

Anchoring.

In the main mechanism considered, the carbocation Pol$^{\oplus}$ attracts a new TFSI$^{\ominus}$ anion, and these two bind strongly without barrier

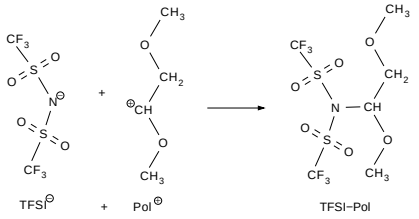

$$\text{M06-HF}: \quad \Delta E = -1.81\ eV$$
$$\text{LC-BLYP}: \quad \Delta E = -1.77\ eV$$

leading to anchoring of a second TFSI$^{\ominus}$ anion to the polymer near the cathode's surface, where ET occurred.

The energy profile for the mechanism is summarized in Figure 2.

The neutral form HTFSI is an extremely strong acid. Once formed, it will likely attack an O from PEO, possibly far from the carbocation. We considered a few possible decomposition products, and found the following to be energetically most favorable:

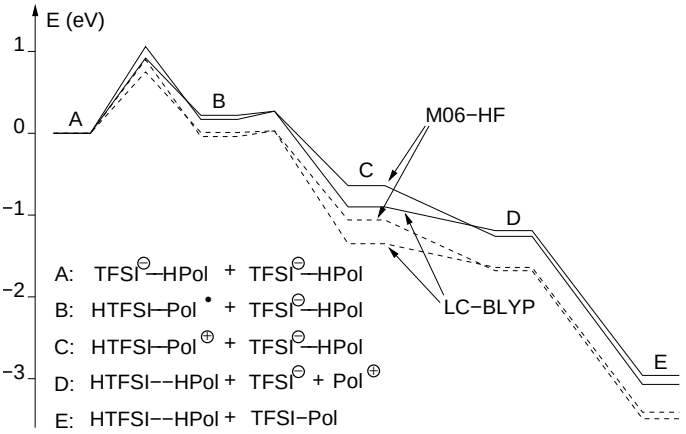

Fig. 2 Energy profile for Path 1 of the proposed mechanism. Solid: before the TP ($\Delta V = 1.06\ V$;) Dashed: at the TP ($\Delta V = 1.27\ V$.) M06-HF and LC-BLYP predict similar profiles, with the 1st step of electrolyte oxidation becoming favorable at or near the TP.

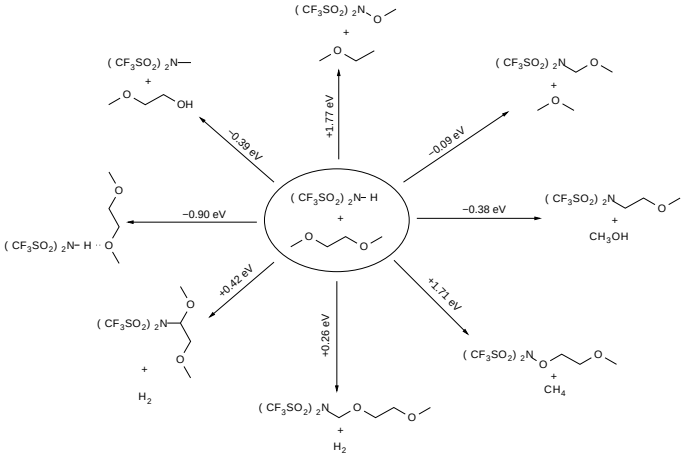

Fig. 3 Possible decomposition steps leading to polymer cleavage and formation of light molecules from HTFSI. The leftmost system represents HTFSI hydrogen-bonded to the polymer.

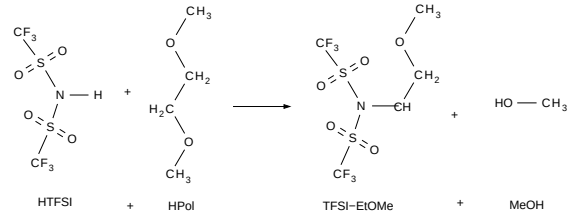

$$\text{M06-HF}: \quad \Delta E = -0.38\ eV.$$

This cleaves the polymer.

Other possible decomposition pathways, involving cleavage in other positions with formation of light molecules, are reported in Figure 3.

As an alternative, HTFSI may migrate to the Li electrode. In

this case it might react with the metal, depending on the SEI:

$$\mathrm{HTFSI} + \mathrm{Li}^{\circ} \longrightarrow \mathrm{TFSI}^{\ominus} + \mathrm{Li}^{\oplus} + \frac{1}{2}\,\mathrm{H_2}$$

which would be detrimental for the battery but observable, in principle, as gas formation near the anode.

1.2 Oxidation of other species

In the reference article by Nakayama et al. the polymer matrix is obtained by radical polymerization from methacrylates of ethylene-oxide olygomers. Presumably, the resulting polymer contains a certain fraction of ester groups, so we computed the IPs of fragments containing these esters near $\mathrm{TFSI}^{\ominus}$ anions. We find that oxidation of the ester is less favorable than the ether, hence oxidation is expected to occur at one of the PEO oxygens.

It should be noted that the systems studied in Ref.[3] include a significant amount of plasticizers, BPEG or APEG. These plasticizers contain B or Al atoms bound to three ethylene-oxide olygomer chains. As the B or Al site of these compounds is a Lewis acid, it may be found near the anions. We investigated the ionization of BPEG. In this case, oxidation of the B center is less favorable than for a PEO oxygen, and we expect the B center to be electrochemically stable. The PEO part of BPEG is expected to behave similarly to the DME considered in the previous section.

Finally, although Nakayama et al.[2,3] did not use alcoholic groups to terminate the polymer chains, OH-terminated PEO is used by other researchers, due to its ready commercial availability. Hence, we studied the oxidation of 2-methoxy ethanol (TME), which form hydrogen bonds with $\mathrm{TFSI}^{\ominus}$. Again, upon oxidation the electron is removed from the ether oxygen, as indicated by Mulliken charges and spin densities, and the IP is the same as for PEO.

We conclude that a PEO oxygen near $\mathrm{TFSI}^{\ominus}$ is indeed the weakest site to be ionized. Numerical details on ester, BPEG, and TME oxidation are reported in the Electronic Supplementary Material.

1.3 Discussion

In summary, the degradation is triggered by an increase in the potential drop ΔV at the cathode/electrolyte interface, which leads to degradation and anchoring of $\mathrm{TFSI}^{\ominus}$. This model predicts an increased electrical resistance near the cathode, due to a lower concentration of charge carriers. Also, the mobility of the remaining $\mathrm{TFSI}^{\ominus}$ and $\mathrm{Li}^{\oplus}$ would decrease, since the TFSI chemically bound to PEO would presumably clog the migration channels. This should increase electrical resistance near the cathode. In turn, the larger resistance would cause an increase in the potential drop ΔV, which would make it even easier to oxidize other PEO sites. Thus, once oxidation begins at one site near the cathode surface, it becomes easier and easier until the catastrophic failure of the battery occurs. We refer to this model of degradation as: Cathode Overpotential Driven Ionization of the Solvent (CODIS)

According to the CODIS model, significant amounts of TFSI would be trapped near the cathode, either chemically bound to PEO, or blocked in PEO regions clogged by anchored TFSI.

Consequences

The CODIS model could be tested in a number of ways.

According to the CODIS model, the average life of a battery should increase if the maximum recharge potential is lowered, for instance from 3.8 to $3.7\,V$. This would certainly lower the cell capacity but it would yield a useful confirmation that degradation starts at the end of the recharging step.

We expect the electrical conductivity of the electrolyte to decrease significantly after the battery failure, especially next to the cathode. This could be measured.

The same ET and degradation could be observed between Pt electrodes separated by PEO-LiTFSI, thus providing accurate measurements of the threshold potential.

Substituting the anion with another that is harder to ionize, for instance $\mathrm{PF}_6^{\ominus}$, should not change significantly the potential at which decomposition occurs, provided the same SEI is formed on the Li surface. But the subsequent degradation path would naturally be different.

Finally, the CODIS model predicts that the ΔV increase at the cathode is a consequence of the decrease from 100 to 70 Ω of the resistance at the Anode/SPE interface. We did not investigate the origin of this decrease, which could be due to

- an increase of the anode surface area (dendrites),
- some curing of the Solid Electrolyte Interface (SEI),
- fluidification of PEO next to the anode, or
- other reasons.

However, regardless of the reason for the improved Anode/SPE performance, re-tuning the cycling voltages as this occurs could prevent degradation.

Alternatively, using a spent anode, with the interface resistance already reduced, coupled with a fresh cathode, could result in a battery recharging at voltages 0.1 to $0.2\,V$ lower than the original, thus preventing degradation while preserving good capacity.

Conclusions

Based on our analysis of the experimental results published by Nakayama et al.,[3] we performed a set of first principles simulations to identify plausible mechanisms for the polymer electrolyte decomposition in PEO-LiTFSI Li-metal rechargeable batteries.

The initial oxidation is likely to occur near the cathode, following a resistance decrease at the anode/electrolyte interface that in turn causes the potential drop across the cathode/electrolyte interface to increase. This first electron transfer from the electrolyte to the cathode involves both one $\mathrm{TFSI}^{\ominus}$ anion and a coordinating polymer molecule and is followed rapidly by a proton transfer and a second oxidation, leading to formation of a strong acidic species and a carbocation. From these species, several decomposition pathways are energetically favorable all of which result in a decreased conductivity near the cathode. Since this reduced conductivity leads to an even larger potential drop at the cathode surface, it favors subsequent decompositions, effectively starting a self-catalytic decomposition reaction.

We call this decomposition model Cathode Overpotential Driven Ionization of the Solvent (CODIS).

We propose a few experimental tests to verify the CODIS model, and suggest possible ways to address the decomposition problem and increase the durability of Li-metal batteries.

Conflicts of interest

There are no conflicts to declare.

Acknowledgements

BVM and WAG thank LGChem and NSF (CBET 1512759) for partial support.

Notes and references

1 Z. Xue, D. He and X. Xie, *J. Mater. Chem. A*, 2015, **3**, 19218–19253.
2 F. Kaneko, S. Wada, M. Nakayama, M. Wakihara, J. Koki and S. Kuroki, *Adv. Funct. Mater.*, 2009, **19**, 918–925.
3 M. Nakayama, S. Wada, S. Kurokic and M. Nogamid, *Energy Environ. Sci.*, 2010, **3**, 1995–2002.
4 C. H. Park, D. W. Kim, P. J. and Y.-K. Sun, *Solid State Ionics*, 2003, **159**, 111–119.
5 M. J. Frisch and al., *Gaussian 09, Revision D.01*, Gaussian, Inc., Wallingford, CT, 2013.
6 K. Raghavachari, J. S. Binkley, R. Seeger and J. A. Pople, *J. Chem. Phys.*, 1980, **72**, 650–54.
7 A. D. McLean and G. S. Chandler, *J. Chem. Phys.*, 1980, **72**, 5639–48.
8 J. Tomasi, B. Mennucci and R. Cammi, *Chem. Rev.*, 2005, **105**, 2999–3093.
9 *CRC Handbook of Chemistry and Physics*, ed. W. M. Haynes, CRC Press, Boca Raton, FL, 95th edn, 2014.
10 N. Koga and K. Morokuma, *Chem. Phys. Lett.*, 1985, **119**, 371.
11 D. R. Yarkony, *J. Phys. Chem.*, 1993, **97**, 4401–4412.
12 M. J. Bearpark, M. A. Robb and H. B. Schlegel, *Chem. Phys. Lett.*, 1994, **223**, 269.
13 J. N. Harvey, M. Aschi, H. Schwarz and W. Koch, *Theor. Chem. Acc.*, 1998, **99**, 95–99.
14 E. R. Fadel, F. Faglioni, S. G., N. Molinari, W. A. Goddard III, B. V. Merinov, J. C. Grossman, J. P. Mailoa and B. Kozinsky, *Submitted*.
15 Y. Zhao and D. G. Truhlar, *J. Phys. Chem. A*, 2006, **110**, 5121–29.
16 Y. Zhao and D. G. Truhlar, *J. Phys. Chem. A*, 2006, **110**, 13126–30.
17 H. Iikura, T. Tsuneda, T. Yanai and K. Hirao, *J. Chem. Phys.*, 2001, **115**, 3540–3544.
18 C. Lee, W. Yang and R. G. Parr, *Phys. Rev.* **B**, 1988, **37**, 785.